Characterization of the Individual Short-Term Frequency Stability of Cryogenic Sapphire Oscillators at the 10^{-16} Level

Christophe Fluhr, Serge Grop, Benoît Dubois, Yann Kersalé, Enrico Rubiola, and Vincent Giordano

***Abstract*—We present the characterization of three cryogenic sapphire oscillators (CSOs) using the three-cornered-hat method. Easily implemented with commercial components and instruments, this method reveals itself very useful to analyze the fractional frequency stability limitations of these state-of-the-art ultrastable oscillators. The best unit presents a fractional frequency stability better than 5×10^{-16} at 1 s and below 2×10^{-16} for $\tau < 5000$ s.**

***Index Terms*—Frequency stability, phase noise, ultrastable oscillators.**

I. Introduction

THE cryogenic sapphire oscillator (CSO) based on a sapphire whispering-gallery mode resonator cooled near 6 K is currently the microwave signal source presenting the highest short-term frequency stability for integration time $\tau = 1 \ldots 10\,000$ s. With a fractional frequency stability better than 1×10^{-15}, the CSO allows the operation of the laser-cooled microwave atomic clocks at the quantum limit [1]. It provides the means to improve the resolution of the space vehicles' ranging and Doppler tracking provided by deep-space networks as well as those of very long baseline interferometry (VLBI) observatories [2]–[7]. The CSO can also enhance the calibration capability of metrological institutes or help the qualification of high performances' clocks or oscillators [1], [8], [9]. The CSO performances are only concurrenced at short integration times ($\tau = 0.1 \ldots 10$ s) by laser stabilized to a room temperature Fabry–Perot (FP) cavity made with low-expansion vitro-ceramic materials [10]–[12]. More recently, fractional frequency stabilities better than 1×10^{-16} have been reported with laser stabilized on cryogenic Silicium FP cavity [13]. Conversely to the CSO, the FP-stabilized laser suffers from a large drift (typically 10^{-12}/day), and requires a femtosecond (FS) laser to deliver the microwave output. In turn, the FS laser is expensive and cumbersome, it can hardly work longer than weeks without loosing internal frequency locking, and suffers from the low signal-to-noise ratio per mode inherent in the wide bandwidth.

Fractional frequency stability better than 1×10^{-15} has already been demonstrated by beating two nearly identical CSOs [14], [15]. The fractional frequency stability of one unit is simply obtained by subtracting 3 dB to the actual result, assuming that the two oscillator noises are equivalent and uncorrelated. This assumption is not generally true especially when developing a new instrument at the state-of-the-art. In our laboratory, we recently achieved the implantation of three nearly identical CSOs in the frame of the Oscillator IMP project. This was the opportunity to test the three-cornered-hat method [16] to extract the individual frequency stabilities. Very preliminary measurements based on this method have been presented in [17]. Since one of the CSOs has been improved and more data have been accumulated. The current results demonstrate the capability of the method, which has been simply implemented with commercial components and counters. Although based on the same general configuration, the three CSOs lightly differ from each other. Different thermal configurations have been tested and only one resonator is completely optimized; the two others recently implemented still need some adjustments. The three-cornered-hat method gives us information about each CSO and thus will help us to optimize its functioning.

II. CSO Description

Our most advanced CSOs incorporate a 54-mm-diameter and 30-mm-height cylindrical sapphire resonator. It operates on the quasi-transverse magnetic whispering-gallery mode $\mathrm{WGH}_{15,0,0}$ near 10 GHz [3]. The Q factor can achieve 1×10^9 at the liquid-He temperature depending on the sapphire crystal quality and on the resonator adjustment and cleaning. In an autonomous cryocooled CSO, the sapphire resonator is placed into a cryostat and in thermal contact with the second stage of a pulse-tube (PT) cryocooler delivering typically 0.5 W of cooling power at 4 K (see Fig. 1). The gas flow in the cryocooler induces mechanical vibrations and a temperature modulation at about 1 Hz, which need to be filtered. In our cryostats, the heat-links between the PT second stage and the flange supporting the 4-K thermal shield and the resonator are made with copper braids or foils. The same mechanical decoupling is implemented between the PT first stage and the 50-K thermal shield. This simple arrangement is sufficient to limit the resonator displacement below 1 μm at the PT cycle

Manuscript received January 10, 2016; accepted March 31, 2016. Date of publication April 4, 2016; date of current version June 1, 2016.

C. Fluhr, Y. Kersalé, E. Rubiola, and V. Giordano are with the Institute Franche-Comté Electronique, Mécanique, Thermique et Optique—Sciences et Technologies (FEMTO-ST), Centre National de la Recherche Scientifique (CNRS), 25000 Besançon, France (e-mail: christophe.fluhr@femto-st.fr; yann.kersale@femto-st.fr; enrico.rubiola@femto-st.fr; giordano@femto-st.fr).

S. Grop is with the Alemnis GmbH, 3602 Thun, Switzerland (e-mail: serge.grop@alemnis.ch).

B. Dubois is with the Center for Technological Development FEMTO Engineering, 25000 Besançon, France (e-mail: benoit.dubois@femto-st.fr).

Digital Object Identifier 10.1109/TUFFC.2016.2550078

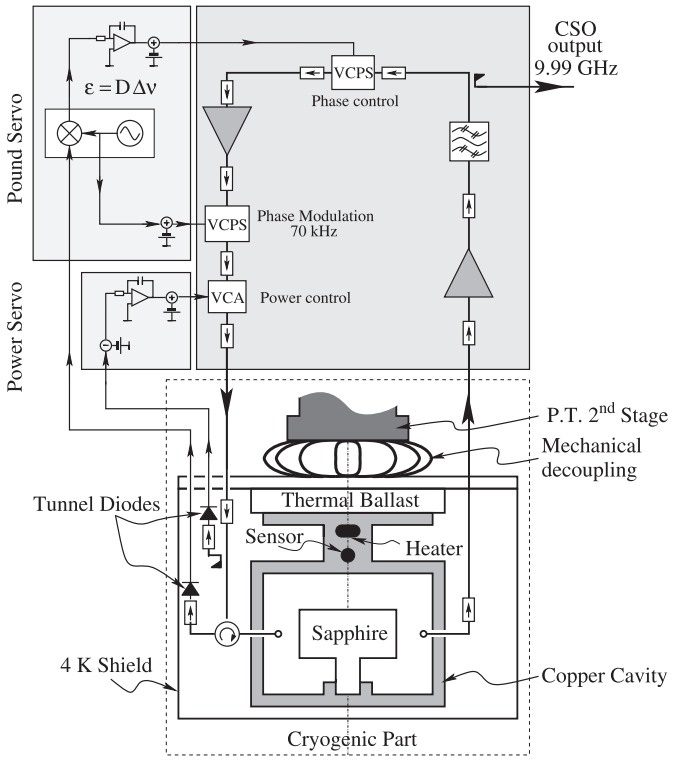

Fig. 1. Scheme of the CSO showing the cryogenic part (cooled resonator) and the electronics placed at room temperature.

frequency [18]. The thermal filtering is obtained by combining the heat-link thermal resistance and the thermal mass of the 4-K flange and its ballast that could be added. Eventually, the resonator is stabilized at its turnover temperature T_0, where its thermal sensitivity nulls at first order. T_0 depends on the residual paramagnetic impurities present in the sapphire crystal [19], and thus is specific to each resonator. T_0 is typically between 5 and 8 K for a high-quality sapphire crystal.

The CSO is a Pound-Galani oscillator [20]. In short, the resonator is used in transmission mode in a regular oscillator loop, and in reflection mode as the discriminator of the classical Pound servo [21]. The sustaining stage and the control electronics are placed at room temperature. The insertion loss through the cryostat is ≈ -30 dB. The sustaining stage is made up of commercial components. Two low-noise microwave amplifiers provide a small signal gain of ca. 54 dB. A voltage-controlled attenuator (VCA) allows the control of the power injected in the resonator. Two voltage-controlled phase shifters (VCPS) are used for the Pound servo. A 70-kHz phase modulation is applied through the first one. The correction is applied through the second VCPS. A 80-MHz bandwidth filter and some isolators complement the circuit. The error signals needed for the Pound and the power servos are derived from the low-frequency voltages generated by two tunnel diodes placed near the resonator input port. The Pound detector is directly connected to a lock-in amplifier (Stanford Research Systems SR 810).

Three oscillators have been assembled successively since 2012. They are identical in the principle but show some differences (see Table I).

The thermal ballast is a piece of stainless steel placed between the PT second stage and the resonator support.

TABLE I
CSOs Main Characteristics

	CSO-1	CSO-2	CSO-3
Resonator			
Frequency ν_0 (GHz)	9.988	9.995	9.987
Material	HEMEX	HEMEX	Kyropoulos
Loaded Q-factor Q_L	1×10^9	3.5×10^8	4.0×10^8
Input coupling coef. β_1	1	1	0.92
Turnover temperature T_0 (K)	6.238	5.766	6.265
Cryostat			
Cryocooler model	PT 405	PT 405	PT 407
Ballast time constant τ_B (s)	12	100	35
Control electronics			
Pound discri. gain D (mV/Hz)	3.4	2.3	1.4
Injected power P_R (μW)	100	300	70

Associated with the thermal resistance of the mechanical link, it is equivalent to a first-order filter with a time constant τ_B.

D is the Pound servo frequency discriminator sensitivity in V/Hz. It depends on P_R: the power injected in the resonator. Formally, D is taken at the demodulator output (see Fig. 1). For slow-frequency fluctuations $\Delta\nu(t)$, the error signal at the demodulator output is $\epsilon(t) = D\Delta\nu(t)$. D is experimentally determined by applying an offset at the lock-in amplifier output and measuring the resulting frequency shift.

CSO-1 is an optimized copy of our first demonstrator, i.e., ELISA developed for the European Space Agency (ESA) and implemented in the deep-space network station DSA-3 in Malargue Argentina [3]. The second one ultra-low instability signal source (ULISS) is a transportable unit, which has been travelled since 2012 in some European laboratories to be tested in real-field applications [14]. The third CSO has a new designed cryostat and was put into operation in October 2014. Not completely optimized, it incorporates a crystal manufactured by the Kyropoulos growth method instead of a HEMEX crystal.

III. Relative Frequency Stability Measurements

The measurement setup is schematized in Fig. 2. The CSO output signals are mixed to obtain the three beatnotes: $\nu_{12} = 7$ MHz, $\nu_{13} = 0.9$ MHz, and $\nu_{23} = 7.9$ MHz. They are simply counted using a multichannels K&K-FXE SCR counter [22]. The three channels work in parallel, thereby the data acquisitions are synchronous. All data are processed by 1-s averaging time using a Λ windowing [23]. The computed two-sample deviation $\sigma_\Lambda(\tau)$ differs from the true Allan deviation $\sigma_y(\tau)$. The correspondence between $\sigma_\Lambda(\tau)$ and $\sigma_y(\tau)$ can be found in [24]. For white and flicker FM noise, these two representations of the fractional frequency stability are almost identical: $\sigma_\Lambda(\tau) \approx 1.14 \times \sigma_y(\tau)$.

A. Beatnotes and Phase Noise

Fig. 3 shows $\sigma_\Lambda(\tau)$ computed from the three beatnotes and compared to the fractional stability of a typical high-performance hydrogen maser (HM.). The bold lines represent $\sigma_\Lambda(\tau)$ without any postdata processing. The thin lines are computed from the data after a linear drift removing.

The measured frequency stabilities are better than 1×10^{-15} for $\tau \leq 2000$ s. If the oscillator noises are equivalent and

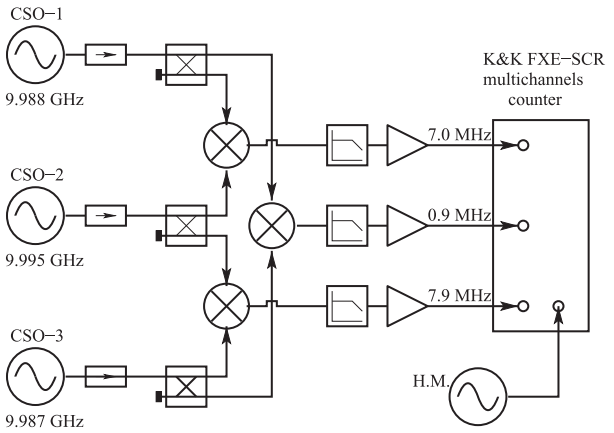

Fig. 2. Measurement setup. Each beatnote is low-pass filtered (10.9 MHz) and amplified (minicircuits ZFL-1000+ amplifier). The multichannel counter is referenced on the 10 MHz coming from an HM.

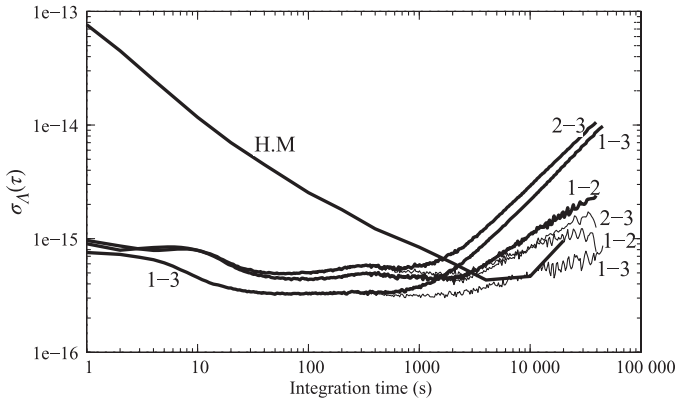

Fig. 3. Two-sample deviations $\sigma_\Lambda(\tau)$ calculated from the three beatnotes.

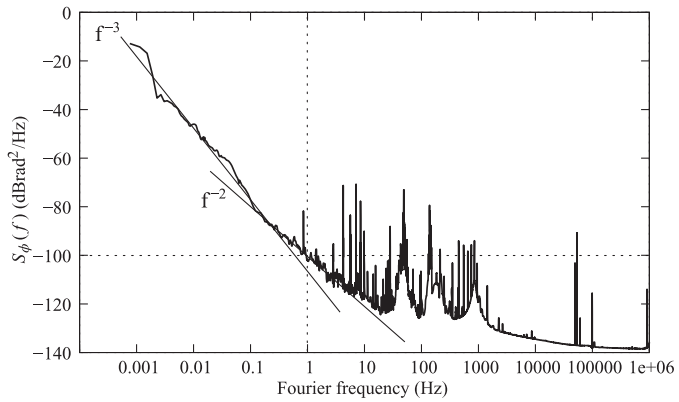

Fig. 4. One unit phase noise obtained by comparing CSO-2 and CSO-3. Measurement realized with the Symmetricom 5125A phase test setup.

uncorrelated, which means that the fractional frequency stability of one unit is better than 7×10^{-16}, which is a conservative value as we will see in the next section. This number is coherent with the phase noise measurement between CSO-2 and CSO-3 shown in Fig. 4.

This result corresponds to the phase noise of one unit assuming equivalent and uncorrelated the two CSOs: 3 dB has been subtracted from the measured spectrum. For Fourier frequency

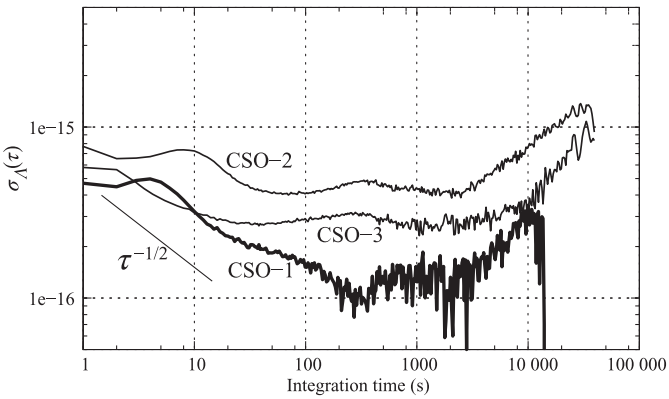

Fig. 5. Individual fractional frequency stabilities obtained by applying the three-cornered-hat method.

$f \leq 10$ Hz, the phase noise spectrum can be approximated by a white frequency noise (f^{-2} slope) and a flicker frequency noise (f^{-3} slope)

$$S_\varphi(f) \approx \left(\frac{1}{f^{-2}} + \frac{0.2}{f^{-3}}\right) \times 10^{-10}\text{rad}^2\text{Hz}^{-1}. \quad (1)$$

This phase noise spectrum is equivalent in the time domain to a deviation $\sigma_\Lambda(\tau)$ such as [25]

$$\sigma_\Lambda(\tau) = 8.2 \times 10^{-16}\tau^{-1/2} + 6.0 \times 10^{-16}. \quad (2)$$

It should be noted that the CSO white PM noise $S_\varphi(f) \approx 10^{-14}$ rad^{2}Hz^{-1} is filtered by the Λ-averaging [24]. This will not be the case with a traditional Π-counter. Thus, the Allan deviation will appear limited at short integration times to $9 \times 10^{-15}\tau^{-1}$, due to the integration of the white PM noise over the counter input bandwidth of 10.9 MHz.

CSO-1 and CSO-3 present the best performances at short term, whereas a perturbation near $\tau = 10$ s affects CSO-2. The long-term behaviors also differ: CSO-1 and CSO-2 do not show a frequency drift but seems limited by a random walk process. Conversely, CSO-3 is drifting with a rate of 2–3$\times 10^{-14}$/day.

B. Three-Cornered-Hat Method

The individual frequency stabilities have been computed using the three-cornered-hat method implemented in the Stable32 software. The results are given in Fig. 5.

At short term ($\tau < 50$ s), all the individual $\sigma_\Lambda(\tau)$ improve with the integration time but do not follow the expected $\tau^{-1/2}$ slope. Indeed, it is expected that the CSO short-term frequency stability is ultimately limited by the Pound discriminator white frequency noise. For CSO-1 and CSO-2, this white frequency noise is completely masked by another process leading to a hump in $\sigma_\Lambda(\tau)$. In Section IV-A, we show that this perturbation can be attributed to residual resonator temperature fluctuations. At longer integration times, the frequency stabilities reach an apparent flicker floor expanding over approximately two decades. Thus for the best oscillator, i.e., CSO-1, $\sigma_\Lambda(\tau) \approx 1.5 \times 10^{-16}$ for 100 s $\leq \tau \leq 5,000$ s.

The humps appearing at $\tau \sim 400$ s can be attributed to an oscillation in the air-conditioning system of the laboratory. Thus, they reveal the residual sensitivity to the room

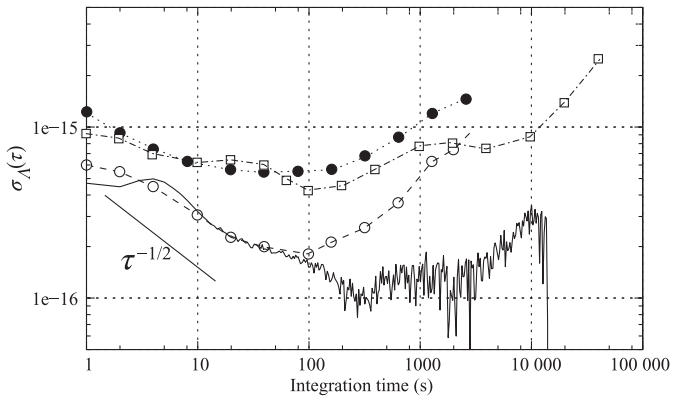

Fig. 6. CSO-1 fractional frequency stability compared previous results: □ V. Giordano *et al.* [14]; • Locke *et al.* [26]; ○ J.G. Hartnett *et al.* [15].

temperature of each CSO. Nevertheless, the resulting CSO frequency variations are obviously correlated, which is in conflict with the requirement of the three-cornered-hat method. The calculated $\sigma_\Lambda(\tau)$ near 400 s cannot be considered as the actual frequency stability. Correlated noises indeed induces false results: the inversed hump in the CSO-1 stability is symptomatic of this situation. The same caution must be taken in the analysis of the long-term fluctuations, resulting also for a large part from the room temperature variations.

IV. Short-Term Frequency Stability Analysis

In Fig. 6, the fractional frequency stability of CSO-1 is compared to the most advanced CSO performances previously published [14], [15], [26]. These ones have been evaluated using the beatnote between two assumed equivalent CSOs.

In [26], Locke describes a liquid helium-cooled CSO. The power injected in the resonator is higher than those used in our devices. Depending on the input resonator port coupling, he evaluates the optimum injected power between 6 and 60 mW. We do not share this approach. In our CSOs, the injected power is much lower, i.e., $P_R \sim 100$ μW. It is set to the value for which the resonator power sensitivity is minimized [27] and thus is specific to each resonator. Locke measured the intrinsic noise of the Pound frequency discriminator. The resulting frequency stability limitation was evaluated to $2 \times 10^{-16}\tau^{-1/2}$, which is well below the observed value. It also demonstrated that the CSO frequency stability is affected by amplitude modulation (AM)-index fluctuations of the interrogation signal. Such a sensitivity makes mandatory a supplementary control loop to suppress the spurious AM. In our CSOs, we do not implement an AM suppression lock loop as we have never highlighted such a strong sensitivity.

In [15], Hartnett describes a cryocooled CSO where the injected power is set to 100 μW. He claims a fractional frequency stability limited by a white frequency noise process. However, it is obvious from Fig. 6 that $\sigma_\Lambda(\tau)$ does not follow the expected $\tau^{-1/2}$ slope for $\tau \approx 1$ s.

From the data presented in Fig. 6, it is clear that there still exist some sources of fluctuation responsible for a frequency stability degradation with respect to the Pound servo intrinsic noise.

A. Noise in the Resonator Temperature Control

The resonator is stabilized at its turnover temperature T_0 using a LakeShore 340 Temperature Controller in the proportional–integral (PI) mode. The temperature sensor is a Cernox type CX-1050 with a sensitivity of approximately 3 kΩ/K. The controller drives a current I_H in a 25-Ω heater. The LakeShore controller makes 10 readings per second and offers a variety of digital processing that can be done to the raw sensor data before applying the PI control equation. Thus, the input information can be in sensor unit (Ω) or converted in temperature unit (K).

The measurement resolution deduced from the LakeShore 340 User's Manual is $\delta R = 1\ \Omega$ equivalent to $\delta T = 300$ μK for the sensor we used. The same datasheet indicates a *control stability* equal to $\pm 2\ \Omega$ (or equivalently ± 600 μK) without any information about the considered bandwidth and the type of noise (white and/or flicker?) affecting the temperature control. Near T_0, the residual thermal sensitivity of the CSO frequency is

$$\frac{1}{\nu_0}\frac{\Delta\nu}{\Delta T} = 1.9 \times 10^{-9}(T - T_0). \tag{3}$$

A rough estimation of the noise floor imposed by the temperature controller can be done by assuming $(T - T_0) \sim \delta T$ and an rms temperature fluctuation $\Delta T \sim 600$ μK. The resulting fractional frequency stability is $\sim 3.4 \times 10^{-16}$. This shows that below a fractional frequency stability of 1×10^{-15}, the noise of the temperature controller has to be considered. A temperature stability of some hundreds of microKelvin is a common performance for such a cryogenic configuration based on a commercial controller and a thermistor [28]–[30]. Better temperature stability of a few μK has been reported on systems using ac-resistance bridge and custom electronic design [31], [32]. Such a solution should be envisaged to improve the CSO short frequency stability and reach the limit imposed by the noise of the Pound frequency discriminator.

We do not know the details of the algorithms implemented in the controller. We checked that for small departures from the temperature setpoint, the Model 340 behaves like a traditional PI controller. If $\epsilon(t)$ is the error signal expressed in Kelvin, the output current I_H can be written as

$$I_H(t) = GP\left[\epsilon(t) + \frac{1}{\tau_I}\int \epsilon(t)dt\right]. \tag{4}$$

G is an internal gain which depends on the controller configuration and on the sensor sensitivity. In our case, we measured $G = 22.5$ mA/K and $G = 1.7$ mA/K when the controller works in sensor unit and temperature unit, respectively. P is the dimensionless proportional gain. τ_I is the integral time [33]. Both P and τ_I can be adjusted from the controller front panel. With the input data processing chosen, the setting of PI-controller gains is done using the autotuning procedure of the LakeShore controller. To start the autotuning, we adjusted the initial values of P and τ_I to those determined by a manual Ziegler–Nichols procedure. Eventually, P and τ_I can be slightly varied by checking the short-term frequency stability and searching for the best result. Fig. 7 shows $\sigma_\Lambda(\tau)$ calculated

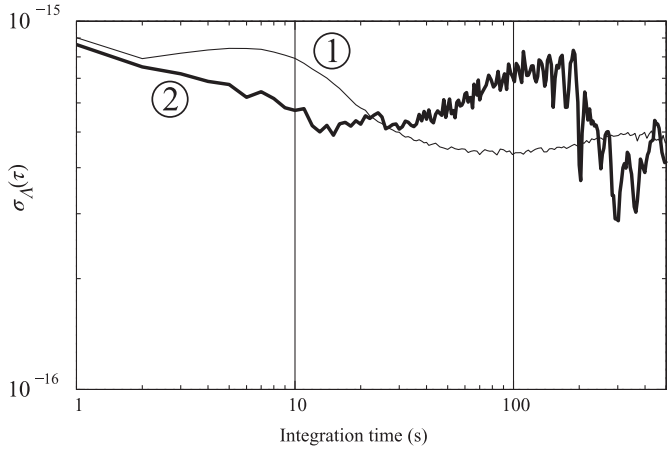

Fig. 7. $\sigma_\Lambda(\tau)$ calculated from the beatnote CSO-1 versus CSO-2, for two temperature controller configuration. 1) Reading in sensor unit (Ω). 2) Reading in temperature unit (K).

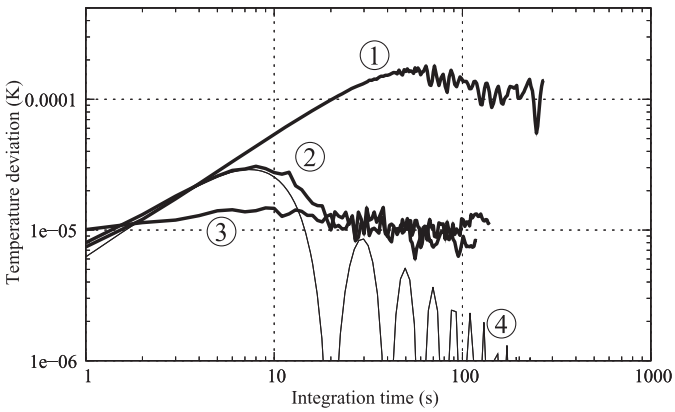

Fig. 8. CSO-1 resonator temperature deviation $\sigma_T(\tau)$ for some temperature controller configurations, the proportional gain is kept constant $P = 300$. 1) Reading in temperature unit (K) , $\tau_I = 16$ s. 2) Reading in sensor unit (Ω), $\tau_I = 16$ s. 3) Reading in sensor unit (Ω), $\tau_I = 8$ s. 4) Computed temperature deviation for a time-varying temperature as: $T(t) = \langle T \rangle + \Delta T \sin(2\pi \frac{t}{\theta_m})$ with $\Delta T = 4 \times 10^{-5}$ K and $\theta_m = 20$ s.

from the beatnote between CSO-1 and CSO-2 for two different configurations of the CSO-2 temperature controller: reading in sensor unit (Ω) or in temperature unit (K). The same P and τ_I are used for both. The effect on the frequency stability is obvious: the hump maximum is shifted to longer integration times when the reading is made in Kelvin with all other parameters being kept constant.

In a second time, we intentionally operate CSO-1 far from its turnover temperature, i.e., at $T = T_0 + 100$ mK. At this point, the first-order resonator temperature sensitivity is $\frac{1}{\Delta T}\frac{\Delta \nu}{\nu_0} = 1.9 \times 10^{-10}/\text{K}$. Thus, the CSO frequency fluctuations will follow those of the resonator temperature. Fig. 8 shows the resonator temperature deviation, i.e., $\sigma_T(\tau)$, for different temperature controller configurations.

The curve 4 is the computed temperature deviation, assuming a resonator temperature modulated around its mean value $\langle T \rangle$ with a period $\theta_m = 20$ s and an amplitude $\Delta T = 4 \times 10^{-5}$ K, which represents well the actual behavior of the configuration 2. The curve 3 corresponds to the best configuration we

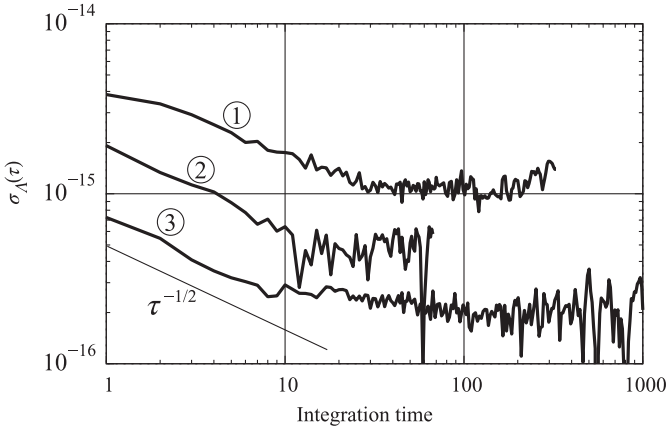

Fig. 9. CSO-3 frequency stability extracted from three-cornered-hat method. The frequency discriminator gain D being 1) 1.3×10^{-4} V/Hz, 2) 3.5×10^{-4} V/Hz, and 3) 1×10^{-3} V/Hz.

found and that has been used for the measurements presented in the previous section. The curve 3 is just above the resolution measurement limited by the frequency noise of CSO-2. The temperature modulation is still there leading to the hump in the CSO-1 fractional frequency stability curve (see Fig. 5). In spite of all our efforts, we did not manage to find a better tuning for CSO-1 and CSO-2. CSO-3 behaves better as no hump has been observed in its $\sigma_\Lambda(\tau)$ curve.

The cause of this temperature modulation as well as its impact on the CSO frequency stability is still not well understood. A modulation amplitude as $\Delta T = 4 \times 10^{-5}$ K will lead to a frequency instability of 5×10^{-16} if the resonator temperature is 6 mK above or below its turnover value T_0. Such an error on the temperature setpoint seems not realistic as it is much higher than the controller measurement resolution of 300 μK. Moreover, we tried to adjust the temperature setpoint by step of 1 mK around the expected T_0 without finding any better tuning. The temperature modulation could result from an unexpected time lag in the thermal system making the control loop unstable. CSO-1 and CSO-2 are operating for a long time. They have been subjected to several stops, and both have been transported by car in the frame of the ULISS project. Thermal anchorages and bold tightenings into the cryostat could have been degraded by the resulting mechanical perturbations. That is coherent with the fact that CSO-3 is immune to these thermal perturbation as it was recently assembled and has not been transported.

B. Noise in the Frequency Discriminator

As explained in the previous section, CSO-3 is the only one not limited at short term by the resonator temperature fluctuations. Its fractional frequency stability is shown in Fig. 9 for several values of the Pound frequency discriminator gain D. The latter has been simply varied by changing the power P_R injected into the resonator, all the other parameters being kept constant.

The measured frequency stabilities follow a $\tau^{-1/2}$ slope until $\tau \approx 30$ s and then a flicker floor. Both vary with the incident power indicating that the CSO-3 performance is limited by the intrinsic noise of the Pound frequency discriminator. In the

TABLE II
COMPUTED VOLTAGE WHITE NOISE SPECTRAL DENSITY e_n

Curve in Fig. 8	$\sigma_\Lambda(1\text{s})$ $\times 10^{-15}$	P_R (μW)	D $\times 10^{-4}$(V/Hz)	e_n (nV/$\sqrt{\text{Hz}}$)
①	5	12,5	1.3	8.0
②	2	33	3.5	8.6
③	0.7	87	9.3	8.0

presence of a white voltage noise at the demodulator output, the CSO short-term fractional frequency stability is [24]

$$\sigma_\Lambda(\tau) = \sqrt{\frac{2}{3}}\frac{e_n}{D\nu_0}\tau^{-1/2} \tag{5}$$

where e_n (V/$\sqrt{\text{Hz}}$) is the demodulator output voltage spectral density. The computed values of e_n are given in Table II.

The constant value $e_n \approx 8$ nV/$\sqrt{\text{Hz}}$ is the equivalent voltage noise of the Pound detector. The direct measurement of e_n requires to duplicate the Pound detector and thus to place a second cryogenic diode receiving the signal reflected by the cavity. This has not been foreseen in our current CSO design. However, this value is compatible with the expected noise contributions of the lock-in amplifier and of the diode detector itself.

Assuming an identical Pound detector noise for CSO-1 and CSO-2 leads to a short-term frequency stability of $3 \times 10^{-16}\tau^{-1/2}$ and $4.4 \times 10^{-16}\tau^{-1/2}$, respectively. For these two CSOs, the Pound discriminator noise is not the dominant process.

V. SUMMARY

We applied the three-cornered-hat method to measure the individual fractional short-term frequency stability of three CSOs. This method implemented with commercial instruments and softwares permits a comparison at the 10^{-16} level. The method also reveals that there still exist technical sources of fluctuation responsible for a degradation of the oscillator frequency stability with respect to the Pound servo intrinsic noise. These perturbations could be minimized by a careful optimization of the thermal system and of the resonator temperature stabilization. Despite these perturbations, all the tested CSOs present a short-term frequency stability better than 7×10^{-16} at 1 s and than 5×10^{-16} between 30 and 3000 s. The best CSO shows a frequency stability of 4.6×10^{-16} at 1 s and a flicker floor below 2×10^{-16}.

ACKNOWLEDGMENT

This work has been realized in the frame of the Agence Nationale de la Recherche (ANR) Project Equipex Oscillator IMP. The Oscillator IMP Project funded in the frame of the French national *Projets d'Investivement d'Avenir* (PIA) targets at being a facility dedicated to the measurement of noise and short-term stability of oscillators and devices in the whole radio spectrum (from MHz to THz), including microwave photonics. The authors would like to thank the Council of the Région de Franche-Comté for its support to the *Projets d'Investissements d'Avenir* and the Fonds Européen de Développement Economique et Régional (FEDER) for funding one CSO.

REFERENCES

[1] G. Santarelli *et al.*, "Quantum projection noise in an atomic fountain: A high stability cesium frequency standard," *Phys. Rev. Lett.*, vol. 82, no. 23, pp. 4619–4622, Jun. 1999.
[2] G. J. Dick, D. G. Santiago, and R. T. Wang, "Temperature compensated sapphire resonator for ultra–stable oscillator capability at temperatures above 77K," *IEEE Trans. Ultrason., Ferroelectr., Freq. Control*, vol. 42, no. 5, pp. 812–819, Sep. 1995.
[3] S. Grop, *et al.*, "ELISA: A cryocooled 10 GHz oscillator with frequency stability," *Rev. Sci. Instrum.*, vol. 81, no. 2, pp. 1–7, 2010.
[4] S. Grop, *et al.*, "Frequency synthesis chain for the ESA deep space network," *Electron. Lett.*, vol. 47, no. 6, pp. 386–388, Mar. 17, 2011.
[5] N. Nand, J. Hartnett, E. Ivanov, and G. Santarelli, "Ultra-stable very-low phase-noise signal source for very long baseline interferometry using a cryocooled sapphire oscillator," *IEEE Trans. Microw. Theory Techn.*, vol. 59, no. 11, pp. 2978–2986, Nov. 2011.
[6] S. Doeleman, T. Mai, A. E. E. Rogers, J. G. Hartnett, M. E. Tobar, and N. Nand, "Adapting a cryogenic sapphire oscillator for very long baseline interferometry," *Publ. Astron. Soc. Pac.*, vol. 123, no. 903, pp. 582–595, 2011.
[7] M. Rioja, R. Dodson, Y. Asaki, J. Hartnett, and S. Tingay, "The impact of frequency standards on coherence in VLBI at the highest frequencies," *Astron. J.*, vol. 144, no. 4, pp. 1–11, 2012.
[8] V. Dolgovskiy, *et al.*, "Ultra-stable microwave generation with a diode-pumped solid-state laser in the 1.5-μm range," *Appl. Phys. B*, vol. 116, no. 3, pp. 593–601, 2014.
[9] A. Takamizawa, *et al.*, "Atomic fountain clock with very high frequency stability employing a pulse-tube-cryocooled sapphire oscillator," *IEEE Trans. Ultrason., Ferroelectr., Freq. Control*, vol. 61, no. 9, pp. 1463–1469, Sep. 2014.
[10] J. Millo, *et al.*, "Ultrastable lasers based on vibration insensitive cavities," *Phys. Rev. A*, vol. 79, no. 5, pp. 1–7, 2009.
[11] M. D. Swallows, *et al.*, "Operating a 87 Sr optical lattice clock with high precision and at high density," *IEEE Trans. Ultrason., Ferroelectr., Freq. Control*, vol. 59, no. 3, pp. 416–425, Mar. 2012.
[12] S. Häfner, *et al.*, "8×10^{-17} fractional laser frequency instability with a long room-temperature cavity," *Opt. Lett.*, vol. 40, no. 9, pp. 2112–2115, May 1, 2015.
[13] T. Kessler, *et al.*, "A sub-40-mHz-linewidth laser based on a silicon single-crystal optical cavity," *Nat. Photon.*, vol. 6, no. 10, pp. 687–692, Sep. 9, 2012.
[14] V. Giordano, *et al.*, "New generation of cryogenic sapphire microwave oscillator for space, metrology and scientific applications," *Rev. Sci. Instrum.*, vol. 83, no. 8, pp. 1–6, 2012.
[15] J. G. Hartnett, N. R. Nand, and C. Lu, "Ultra-low-phase-noise cryocooled microwave dielectric-sapphire-resonator oscillators," *Appl. Phys. Lett.*, vol. 100, no. 18, pp. 1–4, 2012.
[16] J. Gray and D. Allan, "A method for estimating the frequency stability of an individual oscillator," in *Proc. 28th Annu. Symp. Freq. Control*, Fort Monmouth, NJ, USA, May 29–31, 1974, pp. 243–246.
[17] C. Fluhr, *et al.*, "Characterization of a set of cryocooled sapphire oscillators at the 10^{-16} level with the three-cornered hat method," in *Proc. Joint Conf. IEEE Int. Freq. Control Symp. (IFCS) Eur. Freq. Time Forum (EFTF)*, Denver, CO, USA, Apr. 12–16, 2015, pp. 347–350.
[18] S. Grop, P. Y. Bourgeois, R. Boudot, Y. Kersalé, E. Rubiola, and V. Giordano, "10 GHz cryocooled sapphire oscillator with extremely low phase noise," *Electron. Lett.*, vol. 46, no. 6, pp. 420–422, Mar. 18, 2010.
[19] V. Giordano, C. Fluhr, S. Grop, and B. Dubois, "Tests of sapphire crystals manufactured with different growth processes for ultra-stable microwave oscillators," *IEEE Trans. Microw. Theory Techn.*, vol. 64, no. 1, pp. 78–85, Jan. 2016.
[20] Z. Galani, M. Bianchini, R. Waterman, R. Dibiase, R. Laton, and J. Cole, "Analysis and design of a single-resonator GaAs FET oscillator with noise degeneration," *IEEE Trans. Microw. Theory Techn.*, vol. 32, no. 12, pp. 1556–1565, Dec. 1984.
[21] R. Pound, "Electronic frequency stabilization of microwave oscillators," *Rev. Sci. Instrum.*, vol. 17, no. 11, pp. 490–505, Nov. 1946.
[22] G. Kramer and W. Klische, "Multi-channel synchronous digital phase recorder," in *Proc. IEEE Int. Freq. Control Symp. PDA Exhibit.*, 2001, pp. 144–151.
[23] E. Rubiola, "On the measurement of frequency and of its sample variance with high-resolution counters," *Rev. Sci. Instrum.*, vol. 76, no. 5, pp. 1–6, 2005.

[24] S. T. Dawkins, J. J McFerran, and A. N. Luiten, "Considerations on the measurement of the stability of oscillators with frequency counters", *IEEE Trans. Ultrason., Ferroelectr., Freq. Control*, vol. 54, no. 5, pp. 918–925, May 2007.
[25] E. Rubiola, *Phase Noise and Frequency Stability in Oscillators*. Cambridge, U.K.: Cambridge Univ. Press, 2008. ISBN 978-0-521-88677–2.
[26] C. R. Locke, E. N. Ivanov, J. G. Hartnett, P. L. Stanwix, and M. E. Tobar, "Invited article: Design techniques and noise properties of ultrastable cryogenically cooled sapphire-dielectric resonator oscillators," *Rev. Sci. Instrum.*, vol. 79, no. 5, pp. 1–12, 2008.
[27] V. Giordano, S. Grop, P.-Y. Bourgeois, Y. Kersalé, and E. Rubiola, "Influence of the electron spin resonance saturation on the power sensitivity of cryogenic sapphire resonators," *J. Appl. Phys.*, vol. 116, no. 5, pp. 1–7, 2014.
[28] J. G. Hartnett, R. C. Locke, E. N. Ivanov, M. E. Tobar, and P. L. Stanwix "Cryogenic sapphire oscillator with exceptionally high long-term frequency stability," in *Proc. IEEE Int. Freq. Control Symp.*, 2007, pp. 1028–1031.
[29] Y. Huang, J. Weng, and J. Liu, "Experimental investigation on sub-milliKelvin temperature control at liquid hydrogen temperatures," *Cryogenics*, vol. 61, pp. 158–163, May/Jun. 2014.
[30] Y. Hasegawa, D. Nakamura, M. Murata, H. Yamamoto, and T. Komine, "High-precision temperature control and stabilization using a cryocooler," *Rev. Sci. Instrum.*, vol. 81, no. 9, pp. 1–4, 2010.
[31] A. N. Luiten, A. G. Mann, N. J. McDonlad, and D. G. Blair, "Latest results of the UWA cryogenic sapphire oscillator," in *Proc. IEEE Int. Freq. Control Symp.*, 1995, pp. 433–437.
[32] J. Li, J. M. Lockhart, and P. Boretsky, "Cryogenic precision digital temperature control with peaked frequency response," *Rev. Sci. Instrum.*, vol. 75, no. 5, pp. 1182–1187, 2004.
[33] K. J. Åström and T. Hägglund, *Advanced PID Control*. Research Triangle Park, NC, USA: ISA—Instrum. Syst. Autom. Soc., ISBN 978-1-55617-942–6, pp. 64–68.

Christophe Fluhr received the master's degree in microsystem engineering from the Franche-Comté University, Besançon, France, in 2012, with embedded electronics specialization. Since 2015, he has been pursuing the Ph.D. degree in electrical engineering at the Franche-Comté Electronique, Mécanique, Thermique et Optique—Sciences et Technologies (FEMTO-ST) Institute, Besançon, France.

He has been an Electrical Engineer with the Department of Time and Frequency, FEMTO-ST Institute, Besançon, France, since 2013.

Serge Grop received the master's degree in integrated electronics engineering from the Universit Claude Bernard, Lyon, France, in 2005 and the Ph.D. degree in engineering science from the Université de Franche-Comté, Besançon, France, in 2010—in a frame of a European collaboration with the European Space Agency (ESA), Paris, France, the National Physical Laboratory (NPL), Teddington, U.K., and Timetech GmbH, Stuttgart, Germany.

His Ph.D. leads to the development of an ultrastable cryogenic oscillator which is currently running in the ESA Deep Space Station (DSA3), Malargüe, Argentina. In view of these results, he started a commercial activity with his Ph.D. supervisor. From this time, he worked as Technical Manager with ULISS-ST, Besançon, France. In 2015, he joined Alemnis GmbH, Thun, Switzerland, as an R&D Electronic Engineer.

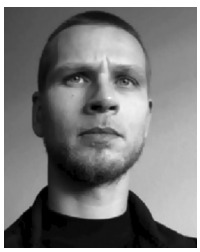

Benoît Dubois received the master's degree in electrical engineering from the Joseph-Fourrier University, Grenoble, France, in 2005, and the Ph.D. degree in electrical engineering from the University of Strasbourg, Strasbourg, France, in 2009.

He has been with the Franche-Comté Electronique, Mécanique, Thermique et Optique—Sciences et Technologies (FEMTO-ST) Institute, Besanon, France, since 2011, first as an Electrical Engineer with the Department of Time and Frequency and currently as an Electrical Engineer with the Technological Center FEMTO Engineering.

Yann Kersalé was born in Rouen, France, on August 16, 1971. He received the Maîtrise degree in theoretical physics from the University of Nantes, Nantes, France, in 1995, and the Ph.D. degree in physical sciences from the University of Franche-Comté, Besançon, France, in 2000.

From 2000 to 2007, he was an Assistant Professor with the University of Franche-Comté, Besançon, France. He is currently a Professor with the Ecole Nationale Supérieure de Mécanique et de Microtechniques (ENSMM), Besançon, France. Since 2000, he has been a Member of the Permanent Staff with the Department of Time and Frequency, Franche-Comté Electronique, Mécanique, Thermique et Optique—Sciences et Technologies (FEMTO-ST) Institute, Besançon, France. His research interests include low-noise microwave oscillators, high-stability cryogenic microwave oscillators for space applications, and ultrastable Fabry–Perot cavities for laser stabilization.

Enrico Rubiola graduated MS degree in electronic engineering from the Politecnico di Torino, Torino, Italy, in 1983, the Ph.D. degree in metrology from the Italian Minister of University and Research, Roma, Italy, in 1989, and the Sc.D. degree in time and frequency from the Université de Franche Comté, Besançon, France, in 1999.

He is a Full Professor with the Université de Franche Comté and Deputy Director with the Department of Time and Frequency of the Centre National de la Recherche Scientifique (CNRS) Franche-Comté Electronique, Mécanique, Thermique et Optique—Sciences et Technologies (FEMTO-ST) Institute, Besançon, France. Formerly, he was a Full Professor with the Université Henri Poincaré, Nancy, France, a Guest Scientist with the NASA JPL, Pasadena, CA, USA, a Professor with the Universitá di Parma, Parma, Italy, and an Assistant Professor with the Politecnico di Torino. He has worked on various topics of electronics and metrology, navigation systems, time/frequency comparisons, and frequency standards. He has developed innovative instruments for AM/PM noise measurement with ultimate sensitivity, and a variety of dedicated signal-processing methods. Since 2012, he has been the PI of Oscillator IMP, a platform dedicated to the measurement of AM/PM noise and short-term frequency stability. His research interests include precision electronics form dc to microwaves and time and frequency metrology including phase and amplitude noise, analog and digital frequency synthesis, high-spectral purity oscillators, photonic systems, sophisticated instrumentation, spectral analysis, and noise.

Vincent Giordano was born in Besançon, France, on February 20, 1962. He received the Engineering degree in mechanics (five-year degree) from the Ecole Supérieure de Mécanique et des Microtechniques, Besançon, France, in 1984, and the Ph.D. degree in physical sciences from the Paris XI University, Orsay, France, in 1987.

From 1984 to 1993, he was a Researcher of the Permament Staff with the Laboratoire de l'Horloge Atomique, Orsay, France, where he worked on a laser diode optically pumped cesium beam frequency standard. In 1993, he joined the Laboratoire de Physique et de Métrologie des Oscillateurs (LPMO), Besançon, France. Institute Franche-Comté Electronique, Mécanique, Thermique et Optique—Sciences et Technologies (FEMTO-ST) was founded in January 2004 from the merger of five different laboratories active in different fields of engineering science: mechanics, optics and telecommunications, electronics, time–frequency, energetics, and fluidics. The Department of Time and Frequency was created in 2006 grouping all the activities related to time and frequency metrology and to micro-acoustics components and systems. His research interests include ultrahigh stability microwave oscillators based on sapphire resonators, microwave and optical atomic clocks, and time and frequency metrology.